

# Signal variation and its morphological correlates in *Paramormyrops kingsleyae* provide insight into the evolution of electrogenic signal diversity in mormyrid electric fish

Jason R. Gallant · Matthew E. Arnegard ·  
John P. Sullivan · Bruce A. Carlson ·  
Carl D. Hopkins

Received: 23 September 2010 / Revised: 18 March 2011 / Accepted: 23 March 2011  
© Springer-Verlag 2011

**Abstract** We describe patterns of geographic variation in electric signal waveforms among populations of the mormyrid electric fish species *Paramormyrops kingsleyae*. This analysis includes study of electric organs and electric organ discharge (EOD) signals from 553 specimens collected from 12 localities in Gabon, West-Central Africa from 1998 to 2009. We measured time, slope, and voltage values from nine defined EOD “landmarks” and determined peak spectral frequencies from each waveform; these data were subjected to principal components analysis. The majority of variation in EODs is explained by two factors: the first related to EOD duration, the second related to the magnitude of the weak head-negative prepotential, P0. Both factors varied clinally across Gabon. EODs are shorter in eastern Gabon and longer in western Gabon. Peak P0 is slightly larger in northern Gabon and smaller in southern Gabon. P0 in the EOD is due to the

presence of penetrating-stalked (*Pa*) electrocytes in the electric organ while absence is due to the presence of non-penetrating stalked electrocytes (*NPP*). Across Gabon, the majority of *P. kingsleyae* populations surveyed have only individuals with P0-present EODs and *Pa* electrocytes. We discovered two geographically distinct populations, isolated from others by barriers to migration, where all individuals have P0-absent EODs with *NPP* electrocytes. At two sites along a boundary between P0-absent and P0-present populations, P0-absent and P0-present individuals were found in sympatry; specimens collected there had electric organs of intermediate morphology. This pattern of geographic variation in EODs is considered in the context of current phylogenetic work. Multiple independent paedomorphic losses of penetrating stalked electrocytes have occurred within five *Paramormyrops* species and seven genera of mormyrids. We suggest that this key anatomical feature in EOD signal evolution may be under a simple mechanism of genetic control, and may be easily influenced by selection or drift throughout the evolutionary history of mormyrids.

**Electronic supplementary material** The online version of this article (doi:10.1007/s00359-011-0643-8) contains supplementary material, which is available to authorized users.

J. R. Gallant (✉) · C. D. Hopkins  
Department of Neurobiology and Behavior,  
Cornell University, Ithaca, NY, USA  
e-mail: jrg63@cornell.edu

M. E. Arnegard  
Department of Zoology, University of British Columbia,  
Vancouver, Canada

J. P. Sullivan  
Museum of Vertebrates, Cornell University, Ithaca, NY, USA

B. A. Carlson  
Department of Biology, Washington University in St. Louis,  
St. Louis, MO, USA

**Keywords** Signal evolution · Geographic variation ·  
Biogeography · Electrocyte · Electric organ

## Introduction

Diversity in courtship signaling behavior is a common component of the evolution of reproductive isolation between species (Mayr 1963). The task of identifying the evolutionary processes that act upon signals to generate such diversity is of considerable interest, and requires insights into the anatomical and physiological basis of signal variation that can be gained through comparative study. For

several reasons, this endeavor is challenging. First, for many communication modalities, signals can be difficult to quantify, particularly in terms of salient aspects relevant to the nervous system and behavior of the organism. Second, it may be difficult to correlate these differences in signals with discrete physiological processes or anatomical differences between species. Third, many courtship signals are subject to a multitude of selective pressures in addition to sexual selection (Bradbury and Verencamp 1998) making it difficult to ascertain the effect of specific evolutionary pressures on communication systems.

We consider here a particularly amenable system for the study of communication signals and species divergence: a species flock of African weakly electric fish. Recent estimates have suggested 22 *Paramormyrops* species (Lavoué et al. 2008). In contrast to the low level of genetic divergence between these species that suggests the recency of their origin (Sullivan et al. 2002), *Paramormyrops* exhibit highly divergent electrical signals (Sullivan et al. 2002, 2004) termed electric organ discharges (EODs). EODs are species-specific, simple, stereotyped, easily quantified signals with a well-established morphological and neurophysiological basis (Hopkins 1986; Carlson 2002; Sullivan et al. 2002; Caputi et al. 2005). The behaviorally salient features of these signals are known (Hopkins and Bass 1981; Carlson 2002), and the neural circuit encoding these features has been well-characterized (Xu-Friedman and Hopkins 1999; Carlson 2009). Moreover, the ease with which EOD waveforms can be quantified permitted a detailed demonstration that these electric signals evolve faster than feeding morphology, size, or trophic ecology implicating sexual selection as a potentially important driving force in mormyrid evolution (Arnegard et al. 2010). Indeed, this has been supported by several playback studies (Hopkins and Bass 1981; Machnik and Kramer 2008; Feulner et al. 2009). This work has motivated our interest in identifying additional evolutionary processes that may lead to the evolution of divergent signals, as well as the anatomical substrates and physiological processes that evolution acts upon to generate signal diversity. Our approach is to use patterns of intraspecific geographic variation as a tool (Mayr 1963; Lewontin 1974; Endler 1989; McPhail 1994; Foster et al. 1998; Verrell 1998) to (1) identify types of variation between populations that parallel signal differences between species and (2) to infer from geographic patterns of this variation, microevolutionary factors that might contribute to signal evolution. Patterns of geographic variation in communication signals, genetics and external morphology have been previously examined for these reasons among the mormyrid genera *Marcusenius* (Kramer et al. 2007; Lamml and Kramer 2007), *Hippopotamyrus* (Kramer et al. 2004; Kramer and Swartz 2010), *Pollimyrus* (Kramer et al. 2003; Lamml and Kramer 2006) and *Petrocephalus* (Kramer and van der Bank 2000).

The present study describes geographic patterns of EOD signal variation in *P. kingsleyae* (Günther 1896), a geographically widespread species in West-Central Africa. EODs are produced by a myogenically derived electric organ, restricted to the caudal peduncle. The mormyrid electric organ is comprised of four axially oriented columns, each consisting of approximately 20–100 disc-shaped electrocytes (Bass 1986b). Interspecific variation in EOD waveforms is explained, in part, by variation in the structure of these electrocytes (Fig. 1; for reviews see also Bennett and Grundfest 1961; Bennett 1971; Bass 1986c). Electrocyte morphology is typically homogeneous across the entire electric organ of an individual (Bass 1986b; Sullivan et al. 2000), and is usually species typical (Sullivan et al. 2000). EODs and electrocyte morphology are especially diverse within *Paramormyrops*; between species EODs may vary in duration (0.5–8 ms), in polarity, in the number of phases, and in the rates of voltage change over time (Sullivan et al. 2002). We focus here on the species *P. kingsleyae*, which exhibits intraspecific EOD diversity (Arnegard and Hopkins 2003; Sullivan et al. 2004; Arnegard et al. 2005). Each EOD type consists of two main peaks, a head-positive phase, P1, followed by a head negative phase, P2. P1 is usually preceded by a weak head negative phase, P0, which is absent in some specimens (Fig. 1). This intraspecific variation is of interest because variation in the presence of P0 versus absence of P0 characterizes much of the diversity in mormyrid EODs, including *Paramormyrops*. In addition, this physiological character has a discrete morphological basis. Mormyrid electrocytes have protruding stalk systems that can originate on the posterior face, and pass through to the anterior face, where they are innervated (*Penetrating* with *anterior* innervation or *Pa*; Fig. 1c). Alternatively they can have stalks that remain on the posterior face, and are innervated on the posterior face (*Non-Penetrating* with *posterior* innervation, or *NPP*; Fig. 1c). The EOD waveform produced by these two electric organ types relates to the direction of current flow through the stalk and the relative order in which the anterior and posterior electrocyte faces depolarize (see Bennett 1971; Bass 1986b). P0-present EODs are associated with *Pa* type electric organs, and P0-absent EODs are associated with *NPP* type electric organs (Fig. 1c).

Our analysis begins with a detailed description of the nature of intraspecific variation in EOD signals of *P. kingsleyae*, followed by a description of the biogeographic patterns that this variation takes. We examine the morphology of electric organs of *P. kingsleyae* from several independent populations, and demonstrate morphological correlates for the observed signal variation. One morphological correlate of signal variation parallels not only interspecific diversity in the *Paramormyrops* species flock, but also within several other genera of mormyrids. We discuss different hypotheses that could potentially explain this variation, and put forward

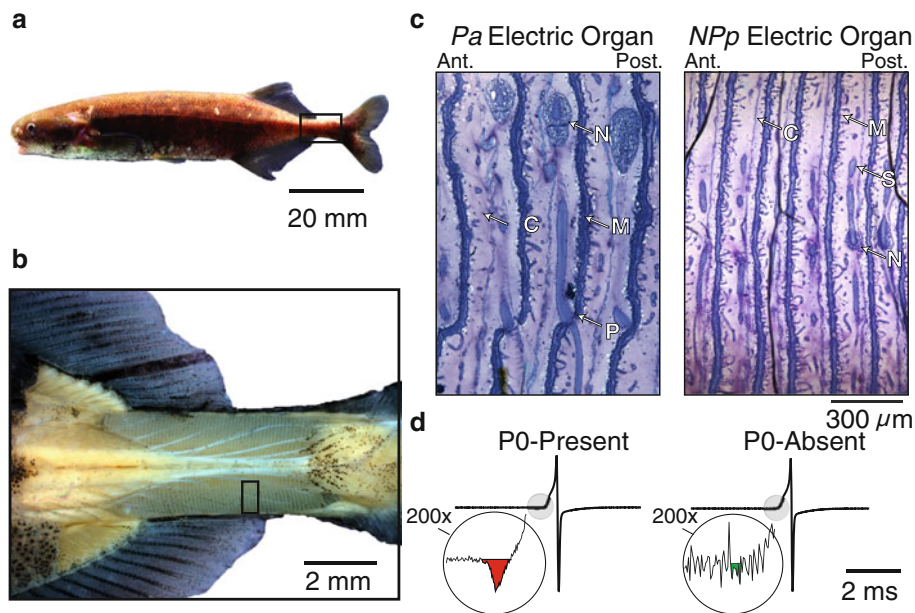


**Fig. 1** *Paramormyrops kingsleyae* and its divergent signaling types. **a** *P. kingsleyae* from Biroundou Creek (see Table 1). **b** The electric organ of *P. kingsleyae* is located in the caudal peduncle. When skin and scales are removed, the electric organ is clearly visible as a striated structure flanked by two groups of muscles. **c** Two specimens are represented by sections of electric organs; *P. kingsleyae* that have either penetrating with anterior innervation (*Pa*) type electric organs or non-penetrating with posterior innervation (*Npp*) type electric organs. Anatomical features

shown are nerve (N), connective tissue septa (C) bounding each electrocyte, microstalklets (M), stalks (S), and penetrations (P). Electrocytes are the dark longitudinal stripes present in each section. For **a–c**, anterior is left, posterior is right. **d** EOD waveforms corresponding to *Pa* and *Npp* type anatomy (above) are shown at  $\times 1$  and  $\times 200$ . A small head negative component at the beginning of the EOD occurs only when *Pa* type electrocytes are present. Mormyrids lacking *Npp* type electrocytes also lack a P0 in their EODs

the hypothesis that genetic drift might play an important role during the early stages of EOD evolution in some mormyrid species in certain geographical settings.

**Methods**

**Specimen collection and electric organ discharge (EOD) recording**

Each of the 553 specimens considered in this analysis are identified as the species *P. kingsleyae*<sup>1</sup> based upon the diagnosis of Hopkins et al. (2007). The Cornell University

Museum of Vertebrates (CUMV) accession numbers (CU80230-95238) with individual voucher numbers (2004-6927), along with collection dates and collection coordinates are listed in tabular format in Online Resource 2. We consider the specimens in this study to be the same species, based upon the following additional evidence: first, 10 of the specimens, representing 10 collection localities listed in the present study, appear to form a monophyletic group within *Paramormyrops*, based on AFLP nuclear genetic markers (Sullivan et al. 2004). Second, the habitat preference of all *P. kingsleyae* specimens is largely for small headwater streams versus main river channels (Table 1). Third, the overall differences between EODs, when compared to intraspecific variation in EODs between other *Paramormyrops*, is quite small (Arnegard et al. 2003; Sullivan et al. 2004), which is the subject of the present study.

*P. kingsleyae* exhibit a sex-difference in their EODs which is evident during the wet-season breeding period with sexually mature males producing EODs approximately double the duration of female and dry season non-breeding males (Bass 1986a; Bass et al. 1986; Bass and Volman 1987). Because of the difficulty of collecting mormyrids from flooded rivers, insufficient samples of exaggerated male EODs have been collected outside of the Ivindo region (Table 1). Given this lack of male recordings, we restrict

<sup>1</sup> *P. kingsleyae* has been previously referred to using several operational taxonomic designators. *Brienomyrus brachyistius* (Long Biphasic or LBP) was used originally by Hopkins (1980), Hopkins and Bass (1981), Bass (1986a, b, c), Bass et al. (1986) and Hopkins (1986). As different regions of Gabon were explored, newly discovered allopatric populations were called *Brienomyrus BNI*, *Brienomyrus BPI*, *Brienomyrus BXI*, *Brienomyrus LIB*, *Brienomyrus CAB* by Sullivan et al. (2002), Arnegard and Hopkins (2003), Sullivan et al. (2004) and Arnegard et al. (2005). Eventually, all of the above populations were recognized as a single species *P. kingsleyae*, on the basis of genetic similarity, similar morphology and ecology, and overall EOD similarity. The most current diagnosis of *Paramormyrops* (formerly “the Gabon-Clade *Brienomyrus*”) and *P. kingsleyae* is summarized by Hopkins et al. (2007), and is provided for convenience as Online Resource 1.

**Table 1** Collections data for all sites and localities

Collection Site	Date	<i>n</i>	Temp (°C)	Cond. (μS/cm)	Lat	Long	Capture	Habitat
<b>Northern Coastal</b>								
<i>Cocobeach</i>								
Small Creek	Mar-00	<b>23</b>	–	52	0°55'57"N	9°34'28"E	N, R	a, 3
Small Creek	Mar-00	<b>7</b>	–	45.7	0°52'14"N	9°35'5"E	N, S	b, 1
<i>Libreville-Cape Estereas</i>								
Small Stream	Feb-98	<b>13</b>	–	71.6	0°33'5"N	9°20'48"E	R	b
Small Stream	Aug-99	<b>2</b>	24.6	31.4	0°35'5"N	9°20'5"E	N, R	b
<b>Ogooué River</b>								
<i>Bambomo</i>								
Bambomo Creek	Jul-99; Aug-09	<b>159</b>	23	13.3–16.3	2°9'49"S	11°27'42"E	R, N	–
<i>Ivindo</i>								
Bale Creek	Feb-98	<b>6</b>	22.8	20.3	0°31'11"N	12°47'58"E	E, N, R	b
Bialé Creek	Jan-98	<b>5</b>	–	–	0°32'18"N	12°49'32"E	N, E, D	–
Nyamé Pendé	Jan-98; Aug-01	<b>4</b>	22.5	17.93	0°30'8"N	12°47'48"E	R	b
<i>Louétsi (Above Falls)</i>								
Louétsi River	Jul-99	<b>6</b>	–	–	2°14'0"S	11°27'0"E	–	–
Banganda Creek	Jul-99	<b>6</b>	21.5	–	2°12'10"S	11°31'45"E	N	–
Bikagala Creek	Jul-99; Aug-09	<b>35</b>	22.1	29.9	2°11'43"S	11°33'40"E	N	–
Songou Creek	Jul-09	<b>11</b>	21.0	14.8	2°16'42"S	11°36'41"E		
Bavelela Creek	Jul-09	<b>23</b>	23	14.4	2°14'33"S	11°33'22"E		
Biroundou Creek	Jul-99; Jul-09	<b>7</b>	24.1	16.03	2°12'47"S	11°28'40"E	N	–
<i>Louétsi (Below Falls)</i>								
Moussabou Creek	Sep-98	<b>8</b>	–	–	2°13'8"S	11°27'50"E	D	–
Apassa Creek	Aug-09	<b>31</b>	22.0	26.0	2°12'42"S	11°27'35"E		
Louétsi River	Sep-98	<b>1</b>	–	–	2°14'2"S	11°27'42"E	H	–
<i>Mouvanga</i>								
Mouvanga Creek	Jul-99; Aug-09	<b>118</b>	21.2–23.8	18.34–23.1	2°19'23"S	11°41'18"E	R, D, N, T	c, a
<i>Niem</i>								
Ngomo River	Sep-99	<b>4</b>	23.3	–	1°42'8"N	11°38'40"E	T, N	–
<i>Nyanga</i>								
Small Stream	Jul-01	<b>4</b>	22.8	–	3°22'27"S	10°47'22"E	–	–
<i>Ogooué</i>								
Small Stream	Sep-01	<b>4</b>	23.8	55.4	0°34'6"S	10°12'47"E	–	3
Diengui River	Sep-99	<b>10</b>	25.5	–	0°39'35"S	10°19'29"E	N	2
Mikouma River	Sep-99	<b>13</b>	26.1	–	0°40'5"S	10°20'12"E	R	a
<b>Okano River</b>								
<i>Okano</i>								
Okano River	Aug-01	<b>38</b>	22.8	21.3	0°49'56"N	11°39'2"E	–	–
<b>Woleu River</b>								
<i>Woleu</i>								
Minka Creek	Aug-99	<b>4</b>	24.2	14	1°32'1"N	11°34'48"E	–	c, 1
Small Stream	Aug-99	<b>11</b>	22	21.3	1°32'41"N	11°45'56"E	R	c, 1

Each of the 26 collection sites are grouped into localities (italic). Major drainages are listed in bold for each of these localities. For each collection site, date visited, number of specimens (N), water temperature, conductivity, Latitude, Longitude, capture type and habitat type are listed. For capture: **N** nets, **R** rotenone, **S** seine, **E** = fishing with detector; **D** = damming, **T** = traps. For habitat: **a** = rocky; **b** = sandy; **c** = muddy; **1** = slow water velocity; **2** = moderate water velocity; **3** = high water velocity. (–) indicates that data are not available

our analysis of electric signal variation to the species-typical female-like EODs exhibited by both breeding females and adult males outside the breeding season. Electrical

playbacks to breeding male *Paramormyrops* spp. suggest that male mate choice targets variable features of these species-typical EODs (Hopkins and Bass 1981; Arnegard

et al. 2006). Playbacks to mormyrids in other genera further suggest that females exhibit mating preferences for variable EOD features in males as well (Machnik and Kramer 2008; Feulner et al. 2009), reinforcing the case that EOD waveforms are an important component of species recognition and mate choice during courtship.

Our collections were made from 26 individual collection sites. For analysis, we grouped these 26 collection sites into 12 regional drainage basins, referred to herein as localities (Table 1). Fish were collected using a variety of methods, including fish traps baited with worms, hand nets and electric fish detectors, hook and line, damming and draining streams (a local fishing technique), and light rotenone applications (Table 1). Following any application of rotenone, fish were immediately transferred to fresh, aerated water, where they recovered completely. We saw no difference in the EODs of rotenone captured fish and those captured using other methods.

EODs of each specimen were originally recorded within hours of capture in 1–5 l plastic boxes filled with water from the collection site. Signals were recorded with bipolar silver chloride coated silver wire electrodes, and amplified (bandwidth = 0.0001–50 kHz) with a differential bioamplifier (CWE, Inc, Ardmore, PA), and digitized at a 100 kHz–1 MHz sampling rate, with head-positivity upward using a Daqbook or WaveBook (IOTECH: Cleveland, OH, USA), or a USB-powered A-D Converter (National Instruments, Austin, TX). All EOD recordings were made at a vertical resolution of 16 bits per sample. After recording their EODs, individual specimens were killed with an overdose of MS-222. We classified obvious mature males based on the presence of an indentation of the body profile along the base of the anal fin (Iles 1960; Okedi 1969; Kirschbaum 1995; Scheffel and Kramer 1997; Pezanzite and Moller 1998). Individuals lacking such an indentation included juveniles and females. Standard lengths were measured from the tip of the snout to the fork of the tail between the two caudal fin lobes (Lévêque et al 1990). Each specimen was given a unique specimen identification tag, and fixed free-floating in 10% formalin (phosphate-buffered; pH 7.2) for at least 2 weeks. Specimens were then transferred to 70% ethanol, and deposited in the Cornell University Museum of Vertebrates. All methods conform to protocols approved by Cornell University's Center for Research Animal Resources and Education.

### EOD analysis

For each specimen, we analyzed a single EOD waveform recording using a custom written program in MATLAB (Mathworks, Inc., Natick, MA), adapted from a previous study (Arnegard and Hopkins 2003). Each EOD waveform

was normalized by its peak-to-peak amplitude, and by subtracting the mean amplitude of the first 100 points. 21 measurements were made on each EOD recording; we measured amplitudes, times and slopes at 9 landmarks defined by peaks, zero crossings, first derivative peaks, and threshold crossings. All landmarks are indicated by red crosses in Fig. 2b and are defined in Table 2 along with a definition of each of the 21 metrics. Slopes at waveform peaks, being zero by definition, were omitted. The zero point of all time measurements was defined by the time of the first head-positive peak (Table 2). We calculated a power spectrum of each EOD waveform using the MATLAB *fft* function to determine the peak frequency and a low and high frequency 3 dB below the peak frequency for each EOD recording. Peak P0 was small in *P. kingsleyae* relative to background electrical noise in recordings, so to measure the magnitude of P0, we integrated the area under the curve between tZC1 and tZC1-0.5 ms (Fig. 2). To obtain a baseline measurement of the noise in each recording, expressed as area, we measured the area under the curve for the first 0.5 ms of each recording (where the EOD is absent). Using the MATLAB function *princomp*, we performed principal components analysis (PCA) on the set of all EOD measurements to quantify EOD signal variation.

Because we describe variation in signals between populations over large geographic areas, we considered differences in recording temperature as a potential confounding source of variation. Kramer and Westby (1985) demonstrated that the overall duration of pulse EODs varied in a manner consistent with a typical  $Q_{10}$  factor of 1.49. In our collections of *P. kingsleyae*, water temperatures at time of EOD recording varied between 21.0 and 26.7°C. Because of incomplete temperature records, we were unable to perform a  $Q_{10}$  temperature correction for each EOD in our analysis. Instead, we evaluated the effect of temperature on a subset of 491 temperature-corrected EOD recordings; the full methodology and results of this analysis are included as Online Resource 3. We concluded from this analysis that recording temperature was not a significant source of variation in our dataset, and therefore proceeded with our analysis on the full ( $n = 553$ ) dataset without temperature correction.

### Electric organ confocal microscopy

We dissected individual electrocytes for whole-mount confocal imaging. Formalin fixation of field-captured specimens (see above) resulted in substantial membrane autofluorescence ( $\lambda = 500$ –550 nm), and such autofluorescence was suitable for confocal imaging of superficial electrocyte structures without further histological processing. Individual electrocytes (approx. 1 mm in dorsal-ventral

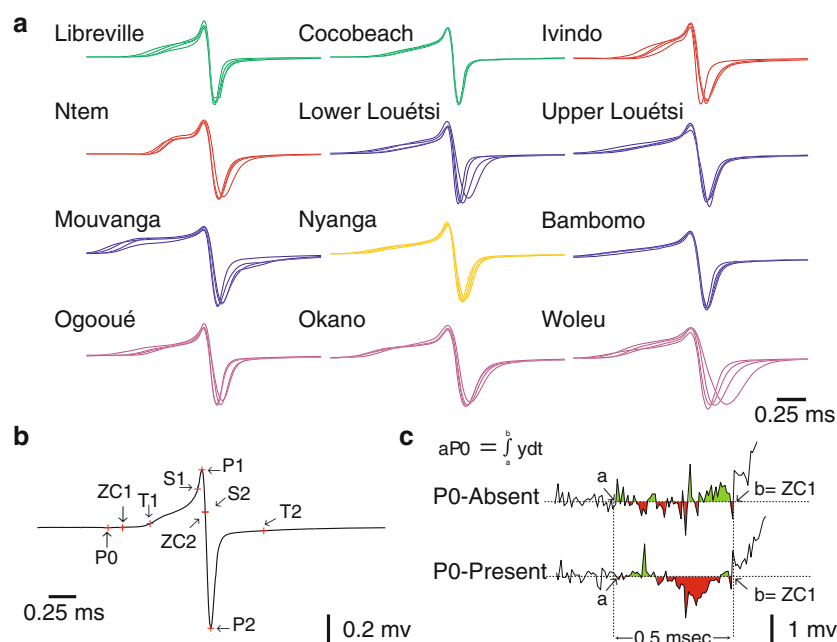


**Fig. 2** EOD waveform analysis of *P. kingsleyae*. **a** Representative variation in EOD waveforms of *P. kingsleyae* from 12 localities ( $n = 4$  EODs for each locality). Waveforms vary principally in the duration and shape of initial P1 phase. **b** Nine landmarks were determined for each of 553 EOD recordings (indicated by red crosses). For each landmark, time and voltage relative to P1 were determined. See Table 2 for definitions of all landmarks used in this

height) were imaged with a Zeiss LSM 510 META microscope using a motorized stage for data collection with optical slices of  $6 \mu\text{m}$ . Laser excitation was at 488 nm; fluorescent emission was collected using a long-pass 505 nm filter and a  $72 \mu\text{m}$  pinhole opening. Slice data from multiple fields of view were assembled for each electrocyte using Zeiss LSM 4.2 software (Carl Zeiss MicroImaging, Thornwood, NY, USA). Resulting stacks were ray-tracer rendered using Volocity 4.5 (Improvision, Waltham, MA, USA) on a white background (1–3% black level, 58% density, 50% brightness). Morphological measurements were performed upon bitmapped versions of electrocyte rendering using a custom-written MATLAB program or IMAGEJ (U. S. National Institutes of Health, Bethesda, MD, USA). We attempted to quantify variation in both the length of microstalklets and in the cross-sectional area of each electrocyte devoted to penetrations by performing image analysis on seven bitmapped 3D projections for which EOD recordings were available. We first determined the area of ellipsoid boundaries surrounding each observed penetration, summed these areas per electrocyte, and then standardized this sum by total electrocyte area. Second, we determined the boundary of each penetration's microstalklets, and then determined linear distances between each pixel in this region to the point of penetration, standardizing this value by the perimeter of the electrocyte.

analysis. **c** P0 is a small pre-potential observed in some waveforms. We determined a robust (even in noisy recordings, as indicated here) method of detection that searches backwards in time from P1 until ZC1 is reached (*b*). The area under the curve is computed for 0.5 ms prior to ZC1 (*a*) to determine P0 area. The time and voltage of the minimum over this interval is recorded as the peak of P0

#### Electric organ light microscopy

We also made serial sections of electric organs for light-microscopy analysis. Electric organs were removed from fixed specimens and decalcified overnight using 100% CalEx-II solution (Fisher Chemicals, Fair Lawn, NJ, USA). Next, tissue samples were dehydrated in a graded alcohol series up to 95%, then infiltrated and embedded in JB-4 glycol methacrylate resin (Polysciences, Inc., Warrington, PA, USA). We then made serial sagittal sections of the embedded samples  $6 \mu\text{m}$  thick, mounted these sections on clean glass slides, and stained each slide with a 0.5% Toluidine blue solution for 30 s. Sections were then imaged using a Leica Leitz DMRB microscope equipped with a SPOT Flex 15.2 64MP Shifting Pixel digital camera (Diagnostic Instruments, Sterling Heights, MI, USA).

For each specimen, we reconstructed one of four columns of electrocytes from serial, sagittal  $6 \mu\text{m}$  sections, cut from lateral to medial. As each column surrounds the spinal cord, we began our reconstruction at the lateral edge of the electric organ, and stopped counting when the spinal cord was clearly visible (approximately  $250\text{--}650 \mu\text{m}$  depending on the size of the individual). For each section, the number of penetrations was counted for each electrocyte (27–72 electrocytes per section) from anterior to posterior. An electrocyte was scored with a penetration

**Table 2** Definitions of landmarks and variables used in PCA analysis of EODs

Name	Definition
<b>Landmarks</b>	
P0	Small negative pre-potential; assumed present in all waveforms
P1	Largest head positive phase
P2	Largest head negative phase
S1	Point of maximum slope between T1 and P1
S2	Point of maximum slope between P1 and P2
T1	Waveform beginning; first point to deviate from baseline by 2% of peak to peak height
T2	Waveform ending; last point to deviate from baseline by 2% of peak to peak height
ZC1	Point voltage crosses baseline from P1-start of record; if exists
ZC2	Point voltage crosses baseline between P1-P2
<b>Variables</b>	
aP0	Area under curve between ZC1-0.5 ms and ZC1
aP1	Area under curve between ZC2-ZC1
aP2	Area under curve between tT2-ZC2
vP0	Minimum voltage between ZC1-0.5 ms and ZC1
vP1	Voltage of P1 ( $vP1 - vP2 = 1$ )
vS1	Voltage at S1
vS2	Voltage at S2
tP0	Time at P0
tP2	Time at P2
tS1	Time at S1
tS2	Time at S2
tZC1	Time at ZC1
tZC2	Time at ZC2
Duration	Total duration ( $T2 - T1$ )
sZC1	Slope at ZC1
sZC2	Slope at ZC2
sS1	Slope at S1
sS2	Slope at S2
fftmax	Peak frequency of FFT transform of EOD
fftlo	Frequency below fftmax at -3 dB
ffthi	Frequency above fftmax at -3 dB

whenever a stalk was observed to pass through either or both faces of the electrocyte (Fig. 1, for example). For our analysis, we considered each 6  $\mu\text{m}$  section to have an independent number of penetrations from all other sections to minimize the probability of underestimating the total number of penetrations.

## Results

### EOD waveform variation

Figure 2 illustrates representative EODs recorded from 48 individuals from 12 different localities across Gabon. EODs vary in duration (e.g. Woleu vs. Cocobeach), in the position of inflection points on the rising phase of the first

peak P1 (e.g. Ntem vs. Lower Louétsi) and in the presence or absence of a small head-negative pre-potential peak, P0, which can be seen on the vertically expanded traces (Fig. 2c). Our quantitative analysis of some aspects of EOD variation is summarized in Table 3 by collection locality. The first two principal components (Fig. 3) of the dataset account for 68.0% of variation in EOD waveform metrics. Principal component 1 describes 48.0% of the dataset variance, and principal component 2 describes an additional 20.0%. Factor loading coefficients for the first two principal components allowed us to determine the combinations of variables that contributed to the majority of variance between waveforms. Variables related primarily to the relative timing of landmarks in the EOD and duration of EOD waveform loaded most strongly on principal component 1, whereas variables related to the

**Table 3** Selected EOD metric values by locality

Locality	<i>n</i>	Duration (ms)	Peak FFT (Hz)	tP0 (ms) <sup>a</sup>	aP0 (mV × ms) <sup>b</sup>
Bambomo Ck	159	1.71 ± 0.35	676.98 ± 135.62	-1.56 ± 0.24	0 ± 0.09
Cocobeach	30	1.37 ± 0.28	957.03 ± 150.42	-1.14 ± 0.18	-0.04 ± 0.11
Ivindo	15	1.47 ± 0.48	917.97 ± 168.34	-0.78 ± 0.13	-0.79 ± 0.45
Libreville	15	1.18 ± 0.2	1,074.22 ± 152.19	-0.79 ± 0.07	-0.2 ± 0.05
Lower Louétsi	40	1.41 ± 0.21	760.5 ± 112.7	-1.22 ± 0.12	-0.31 ± 0.13
Mouvanga	119	1.84 ± 0.22	649.21 ± 91.6	-1.42 ± 0.14	-0.35 ± 0.12
Ntem	4	1.06 ± 0.1	1,074.22 ± 112.76	-0.51 ± 0.04	-0.56 ± 0.13
Nyanga	4	1.5 ± 0.18	756.84 ± 93.5	-1.21 ± 0.09	-0.37 ± 0.07
Ogooué	27	1.49 ± 0.3	788.48 ± 157.76	-1.16 ± 0.17	-0.29 ± 0.11
Okano	38	1.87 ± 0.17	601.36 ± 53.37	-1.32 ± 0.08	-0.43 ± 0.15
Upper Louétsi	87	1.5 ± 0.29	802.02 ± 133.75	-1.49 ± 0.22	0.04 ± 0.13
Woleu	15	1.4 ± 0.15	794.27 ± 103.53	-0.94 ± 0.07	-0.4 ± 0.35
<i>Total</i>	553				

Values for selected variables (see Table 2) are listed by Locality (see Table 1) ± SD

<sup>a</sup> Relative to tP1 = 0 ms

<sup>b</sup> Relative to vP1 - vP2 = 1

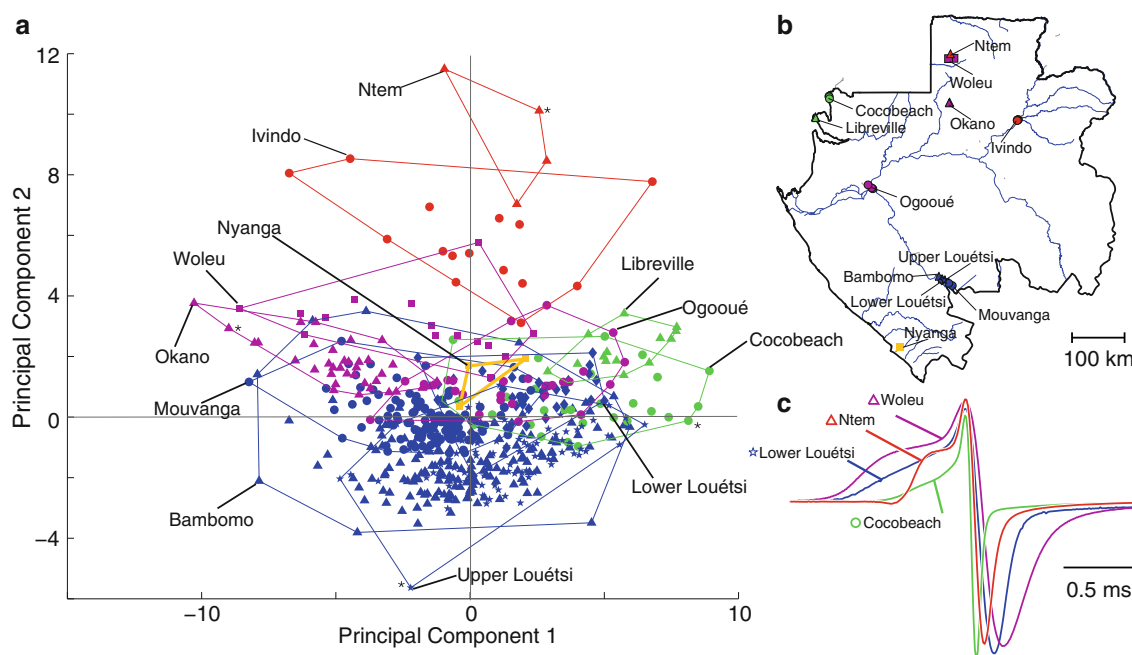


**Fig. 3** Principal components analysis of EOD waveform variation for the *P. kingsleyae* dataset. **a** The first two principal components ( $n = 553$ ) describe variation across 21 variables. Each data point represented in principal component space has a representative shape and color corresponding to locality (**b**). Each locality is bounded by a minimum polygon (colored line, labeled with locality). *Asterisk*

symbols represent the EOD waveforms shown in **c**. **b** Map of Gabon with major rivers; 12 collection localities are shown and shaded by geographic region (*Green* West, *Purple* N. Central, *Red* N. East, *Blue* Southern, *Yellow* Nyanga). Shapes are assigned based on population. **c** Overlay diagram of four EOD waveforms indicated by *asterisks* in **a**

magnitude of P0 loaded most strongly on principal component 2 (Table 4).

Boundaries plotted in Fig. 3 illustrate that variation in EOD waveform is less within localities than between localities. Typically, variation in geographically adjacent

localities is less than geographically distant ones, with the exception of Ntem and Woleu which are geographically proximate, but separate watersheds. To evaluate this relationship more stringently, we examined the correlation between principal components scores 1 and 2 each with

**Table 4** Top ten factor loading values for principal components 1 & 2

Variable	PC1	Variable	PC2
ap2 <sup>a</sup>	0.3058	tZC1	0.4055
ap1 <sup>a</sup>	-0.2984	tP0 <sup>b</sup>	0.3952
ffthi <sup>a</sup>	0.2866	vP0 <sup>b</sup>	-0.3887
sZC2	-0.2811	sZC1	0.3761
duration <sup>a</sup>	-0.2793	ap0 <sup>b</sup>	-0.3578
sS2	-0.2777	vS1 <sup>b</sup>	0.2497
tP2 <sup>a</sup>	-0.2735	ffitlo	0.2308
tZC2	-0.2668	ffitmax	0.2015
tS2 <sup>a</sup>	-0.2630	vS2	0.1559
ffitmax <sup>a</sup>	0.2516	tZC2	0.1337

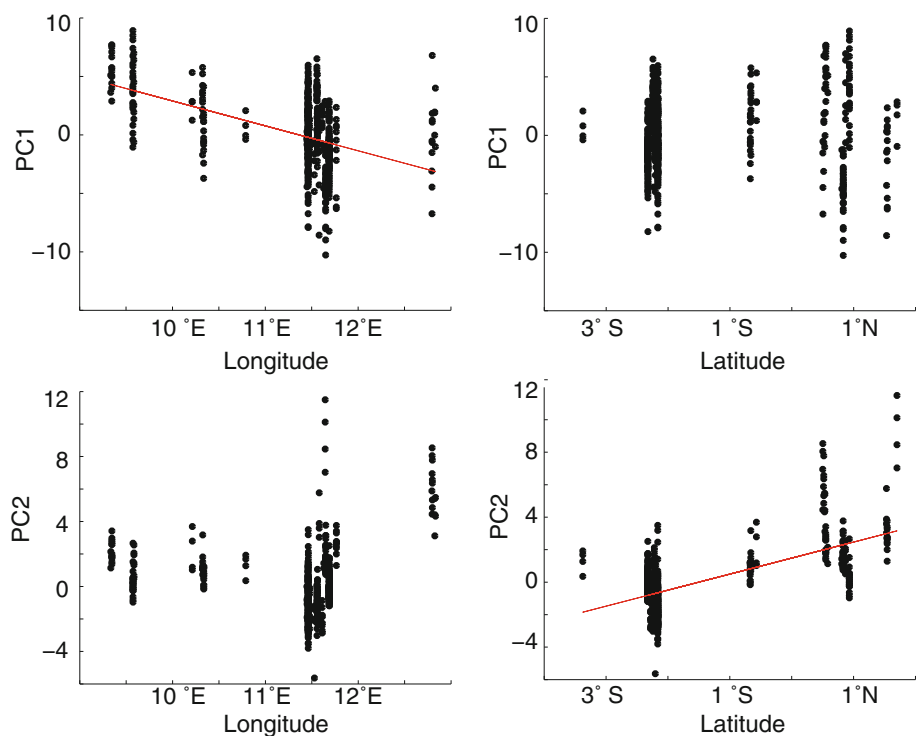
The ten highest-magnitude loading scores for each PC1 and PC2 are shown with their associated variables. The magnitude of the loading score indicates the relative contribution of each individual variable to variation in this principal component

<sup>a</sup> Factors for PC1 which are related to overall duration of EOD waveform

<sup>b</sup> Factors for PC2 which are related to overall magnitude of phase P0 (see Table 1)

latitude and longitude. PC scores are plotted versus longitude and latitude in pairwise combinations in Fig. 4. Linear regression analysis indicated a significant linear relationship of principal component 1 to longitude (slope = -2.13;  $F = 143.98$ ,  $df = 552$ ,  $r^2 = 0.21$ ,  $P < 0.001$ ) but not latitude, and principal component 2 with increasing latitude

**Fig. 4** Clinal variation in EOD waveform. Principal component 1 of all data has a negative linear relationship with Longitude (*upper left*;  $F = 143.98$ ;  $df = 552$   $R^2 = 0.21$ ;  $P < 0.001$ ) but not Latitude; principal component 2 of all data has a positive linear relationship with Latitude (*lower right*;  $F = 387.77$ ,  $df = 552$ ,  $r^2 = 0.41$ ;  $P < 0.001$ ) but not Longitude



(slope = 0.99;  $F = 387.77$ ,  $df = 552$ ,  $r^2 = 0.41$ ,  $P < 0.001$ ) but not longitude.

P0 signal analysis

Figure 5a shows a histogram of all 553 measured P0 areas. Three example waveforms are shown as insets; the EOD on the far left has a P0 area of -0.79 mV × ms, the EOD on the left has a P0 area of -0.17 mV × ms, and the P0-absent EOD on the right has a P0 area of 0.03 mV × ms. The histogram of all individuals is bimodal with respect to their P0 magnitude, representing P0 present individuals (the left modal peak, -0.35 mV × ms), or P0 absent individuals (the right modal peak at 0.00 mV × ms). Because of noise in the recordings, some fish with no discernible P0 had a measurable P0 area when applying this metric. We wished to compare the magnitude of our measured P0s to the noise in our recordings, so we determined the mean value of the area under the curve during the first 0.5 ms (see “Methods”) for all recordings (where no EOD is present). A histogram of these area measurements is shown in Fig. 5b. Next, we classified waveforms as either P0-absent (green) or P0-present (red) using the threshold value 3 standard deviations from this mean value (-0.064 mV × ms). Thus EODs that had a P0 area significantly greater than the area under the curve in the recording noise ( $P = 0.01$ ) were considered P0-present. Those that had a P0 area less than three standard deviations from 0 mV × ms were considered P0-absent. Note that

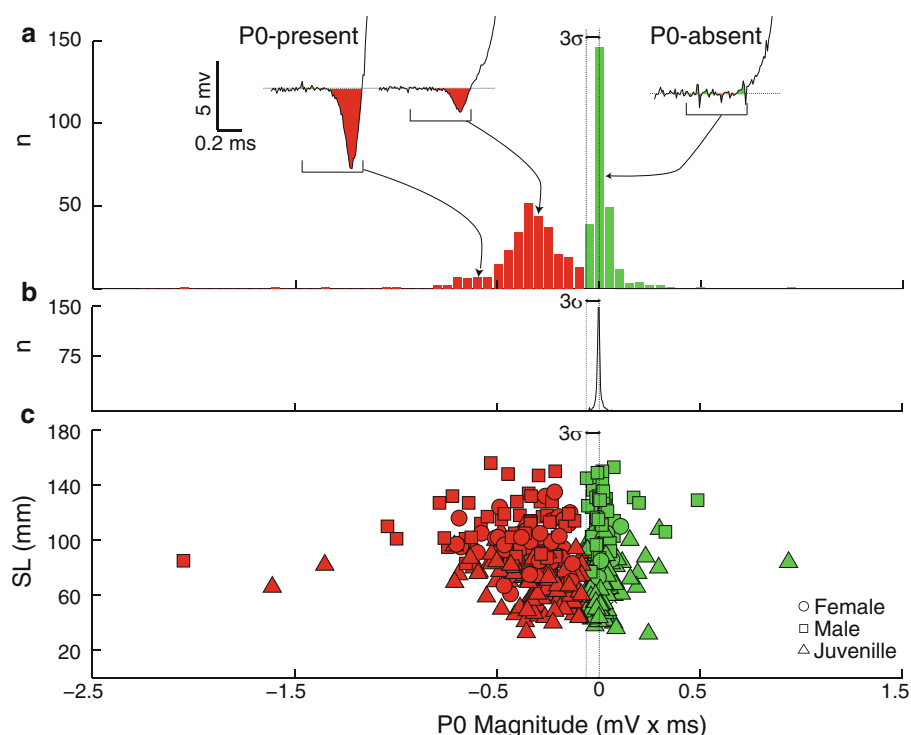


**Fig. 5** Distribution of P0 magnitude among collected *P. kingsleyae* specimens. **a** Histogram of P0 areas ( $n = 553$ ) indicates a bimodal distribution of P0 areas corresponding to P0-present waveforms and P0-absent waveforms. Modal P0 magnitude of P0-present waveforms is  $-0.35 \text{ mV} \times \text{ms}$ , modal value for P0-absent waveforms is  $0.00 \text{ mV} \times \text{ms}$ . *Insets* show representative EOD waveforms; *far left inset* is P0-present ( $\text{P0} = -0.79 \text{ mV} \times \text{ms}$ ), *middle left* is P0-present ( $\text{P0} = -0.17 \text{ mV} \times \text{ms}$ ), *right inset* is P0-absent ( $\text{P0} = 0.03 \text{ mV} \times \text{ms}$ ) **b**. Shown is a histogram of area measurements in the first 0.5 ms of each

recording, where no EOD is present, indicating the area under the curve due to electrical noise in the recordings (see “Methods”). We used the value ( $-0.064 \text{ mV} \times \text{ms}$ ) 3 standard deviations smaller than the mean area of the recording noise (and thus significant at the  $P = 0.01$  level) as a threshold for classifying individuals as P0-absent or P0-present (green and red, respectively). **c** Individual P0 values plotted by sex and standard length (SL) indicate no relationship (see “Results”) between either variable ( $n = 524$ ; for 29 specimens sex or SL were not determined)

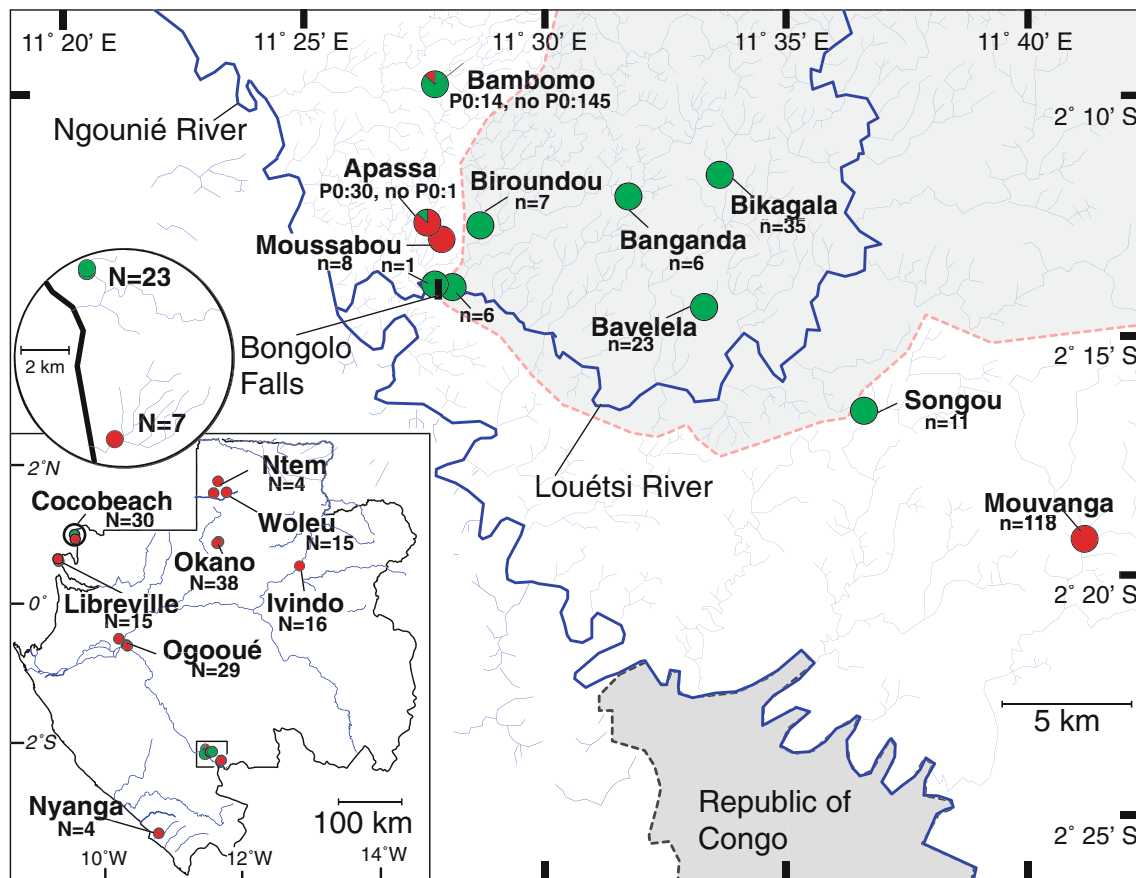
this threshold corresponds exactly to the “trough” between the two modes in the distribution of P0 area across all populations, generating two objectively defined classes of EOD waveforms in *P. kingsleyae*. Accordingly, 297 individuals were classified as P0-present; 256 individuals were classified as P0-absent.

Figure 5c shows P0 area plotted against standard length and sex. There is no significant difference in P0 magnitude between males and females (one-way ANOVA;  $F = 0.01$ ,  $df = 523$ ,  $P = 0.9365$ ). There is a weak but statistically significant linear correlation with standard length, a general indicator of specimen age in fish (slope =  $-0.0012$ ;  $F = 10.76$ ;  $df = 552$ ;  $P = 0.001$ ,  $r^2 = 0.01$ ). P0 area (one-way ANOVA;  $F = 103.31$ ,  $df = 11$ ,  $P < 0.0001$ ) and time of P0 (one-way ANOVA;  $F = 72.44$ ,  $df = 11$ ,  $P < 0.0001$ ) varied significantly among collection localities.

Figure 6 illustrates the geographic distribution of our sampling efforts across Gabon. Pie charts for each collection locality represent the proportion of signal types at each collection site, and sample sizes are listed below. In the majority of localities, only P0-present individuals were captured. P0-absent individuals occurred only in two

geographically distinct regions (Cocobeach, Fig. 6 circular inset, and in the Louétsi drainage basin, Fig. 6). Both signal types were observed at two collection sites: Apassa Creek ( $n = 31$ : 30 P0-present, 1 P0 absent) and Bambomo creek ( $n = 159$ : 14 P0-present, 145 P0-absent).

After the 1998 and 1999 collecting seasons, the combination of data from high-resolution topographic maps, GIS coordinates, and detailed signal analysis revealed that only P0-absent individuals were collected in rivers draining into the Louétsi river above Bongolo Falls (Fig. 6, gray area bounded by red dashed line), and that P0-present individuals were predominantly captured in rivers draining into the Louétsi and Ngounié rivers below Bongolo Falls. We hypothesized that Bongolo Falls acted as a barrier between the two signaling types, and tested this hypothesis with additional sampling in these and additional creeks in 2009. Table 5 summarizes the results of our collecting efforts. Our collections in 2009 were consistent with collections made in 1998–99; the same signaling types were collected at the same sites 10 years later in Biroundou, Bikagala, Bambomo and Mouvanga Creeks. Above Bongolo Falls, only P0-absent individuals were captured



**Fig. 6** Geographic distribution of P0 absent and P0 present *P. kingsleyae* collected 1998–2009. We indicate the distribution of P0 absent and P0 present individuals in Gabon at a variety of geographic scales. Each sampled locality is displayed as a pie chart proportional to signaling types collected. Pie charts are shaded based on signal type; red indicates proportion of *P. kingsleyae* that are P0-present; green indicate proportions of *P. kingsleyae* that are P0-absent. Sample sizes for each population are indicated. The map of Gabon (lower left) represents our sampling efforts across Gabon; the circular inset is a

detailed view of the area known as Cocobeach. The main figure is a detailed view of the area surrounding the confluence of the Louétsi and Ngounié rivers. Two populations (Bambomo and Apassa) were mixed for both P0-absent and P0-present signal types. The *lightly shaded area*, bounded by a *red dashed line*, corresponds to the Upper Louétsi watershed, which is isolated from the Lower Louétsi watershed by the presence of a 15 m waterfall, Bongolo Falls. The *grey shaded area*, bounded by a *grey dashed line*, demarks the boundary of the Republic of the Congo

during these two field seasons. During 2009, we found an exceptional population, Songou creek, where the river drained into the Ngounié River, but had entirely P0-absent individuals ( $n = 11$ ). Two populations had individuals that had both P0-absent and P0-present EODs; Apassa Creek (Surveyed only in 2009) and Bambomo Creek (surveyed in 1998–99 and 2009).

Morphology of electric organs and individual electrocytes

Figure 7 summarizes counts of stalk penetrations in 8 of the 12 electric organs surveyed, exemplifying the variation in electric organ anatomy we observed. Each section surveyed is represented as a square shaded based on the number of penetrations observed (gray = 0; orange = 1;

yellow = 2; red = 3; white = section missing/no data). Each column represents a single electrocyte; each row represents a single 6  $\mu$ m section made from lateral to medial. For each specimen, the number of electrocytes analyzed for each individual is reported ( $n = 27$ –72 electrocytes). Only partial organs were available for Cocobeach 4015 and 4025. In some electric organs, stalk penetrations were present only in a few electrocytes (nearly every column is gray from left to right, e.g. Cocobeach 4002). In others, penetrations are evident in almost every electrocyte (plot has a colored pixel in nearly every column from left to right; e.g. Mouvanga 2627), indicative of *Npp* or *Pa* type morphology respectively. A third group of electric organs had penetrations in some electrocytes, but not others (plot has some columns containing color, and adjacent columns are lacking color in all 6  $\mu$ m sections). Our survey

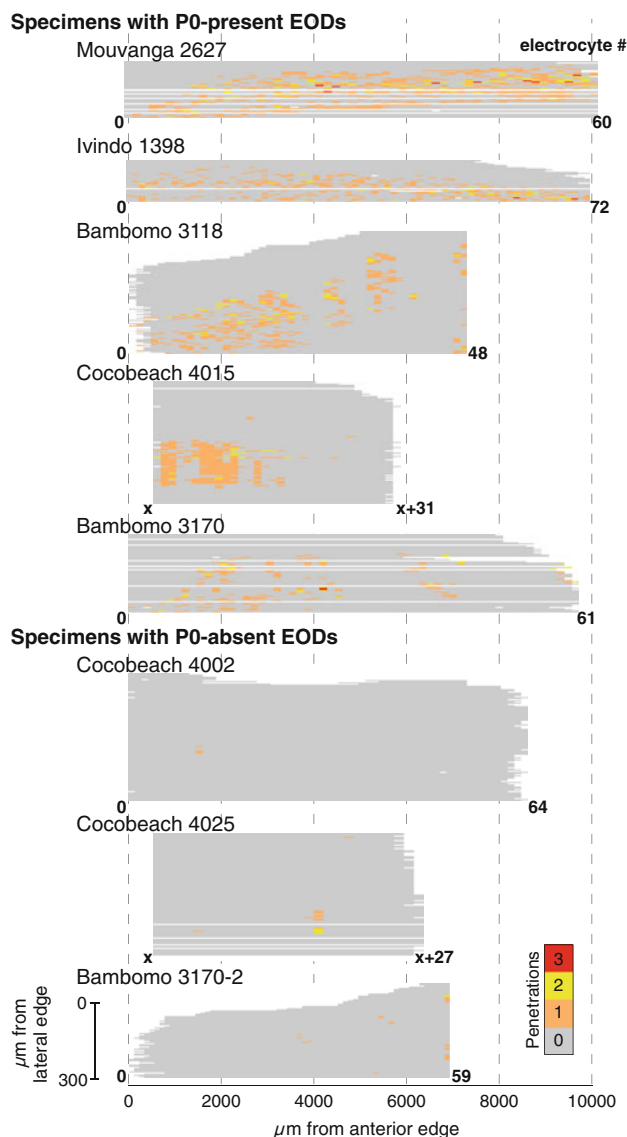
**Table 5** Summary of predominant signaling types in 1998–1999 and 2009 near Bongolo Falls

Site Name	Drainage	1998–99	2009
Biroundou	Above	P0 Absent	P0 Absent
Banganda	Above	P0 Absent	–
Bikagala	Above	P0 Absent	P0 Absent
Bavelela	Above	–	P0 Absent
Louétsi River	Above	P0 Absent	–
Bambomo	Below	Mixed	Mixed
Moussabou	Below	P0 Present	–
Songou	Below	–	P0 Absent
Mouvanga	Below	P0 Present	P0 Present
Louétsi River	Below	P0 Absent	–
Apassa	Below	–	P0 Present

Predominant signal types are noted for each collection locality visited in 1998–1999 and 2009. Sites are described as draining into the Louétsi River above and below Bongolo Falls. Sites that were not surveyed in that year are listed as (–)

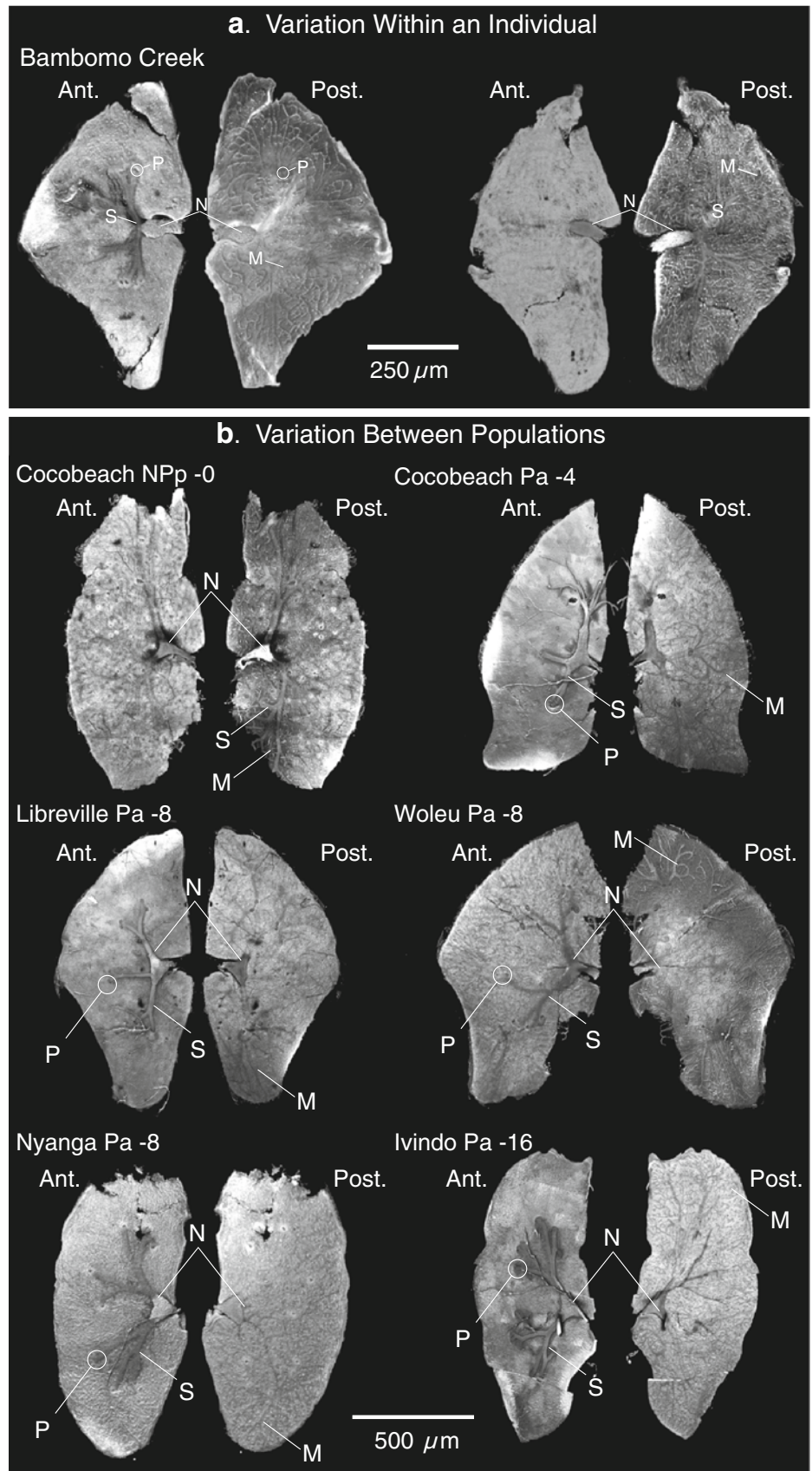
of all 12 electric organs is summarized in Table 6. For each electric organ, the number of penetrations was summed for each electrocyte across all sections. Six specimens examined with P0-present waveforms had predominantly *Pa* type electrocytes, and six specimens examined with P0-absent waveforms had predominantly *NPp* type electrocytes. In six of twelve specimens, we observed both *Pa* and *NPp* electrocytes in the same electric organ.

We also used confocal microscopy to visualize the complex, three-dimensional morphology of an additional eight, individually dissected, electrocytes (see “Methods”). Figure 8a displays confocal 3D reconstruction of the anterior and posterior faces of two electrocytes dissected from one individual that had both electrocyte types, Bambomo specimen number 3118. One electrocyte (Fig. 8a; left) is *Pa*; the other (Fig. 8a; right) is *NPp*. Figure 8b shows the anterior and posterior faces of electrocytes from additional localities. For each electrocyte, morphological features, number of penetrations, and specimen locality are indicated. In *Pa* type electrocytes, the nerve and stalk system are visible on the anterior face, whereas microstalklets, the result of profuse stalk branching following a penetration, fuse over restricted regions of the posterior face (“territories”). In *NPp* type electrocytes, the nerve, microstalklets, and stalk system are only visible on the posterior face. We observed differences in the number of the stalk penetrations (4–16) between electrocytes, as well as in the length of microstalklets on the posterior face of *Pa* type electrocytes. Though these individual electrocytes were selected from electric organs composed of several hundred electrocytes, the number of penetrations detected by this method in each electrocyte



**Fig. 7** Heterogeneous and homogeneous electric organ morphology in *P. kingsleyae*. We show here variation in electric organ morphology from eight individuals, representing three major types of electric organs observed (mostly *Pa*, mostly *NPp* and mixed). Number of penetrations in individual section is indicated by color (gray 0, orange 1, yellow 2, red 3, white section missing/no data). For all plots, horizontal axis represents distance from the anterior edge of the electric organ, and the vertical axis represents distance from the lateral edge of the electric organ (top lateral). Mouvanga 2627 and Ivindo 1398 represent “typical” patterns of penetration in P0-present type Mormyrids. *Pa* type morphology is present in each electrocyte, characterized by a colored box in each column from anterior to posterior. In Bambomo (3170; 3118) and Cocobeach (4015) P0-present specimens the electric organ is heterogeneous (both *Pa* and *NPp* electrocyte morphology). P0-absent specimens (Bambomo 3170-2; Cocobeach 4002, 4025) exhibit comparatively homogeneous *NPp* morphology in the electric organ. Numbers of electrocytes are noted in bold on the ends of each plot; note the variability in the number of electrocytes between individuals. For Cocobeach 4025 and 4015 only a posterior portion each electric organ was available for analysis

**Fig. 8** Confocal reconstruction of within and between specimen variation in electrocyte morphology. For each electrocyte, anterior faces are shown on the *left*, posterior faces on the *right*. For each, the nerve (N), stalk (S), microstalklets (M), and penetrations (P) are shown. **a** Two electrocytes were dissected from the electric organ of a single specimen. Eight penetrations can be observed in the electrocyte on the left, none can be observed in the electrocyte on the right. The *Npp* electrocyte (*right*) is innervated on the posterior face and has microstalklets on the posterior face. No penetrations can be observed, and no stalk is observed on the anterior face. **b** Variation in *P. kingsleyae* electrocytes. Shown are six 3D projections of the anterior and posterior faces of electrocytes from various localities dissected from individual specimens. Cocobeach *Npp* has no penetrations; stalk is located only on posterior face. For all other electrocytes, penetrations are visible, and stalk is located on the anterior face



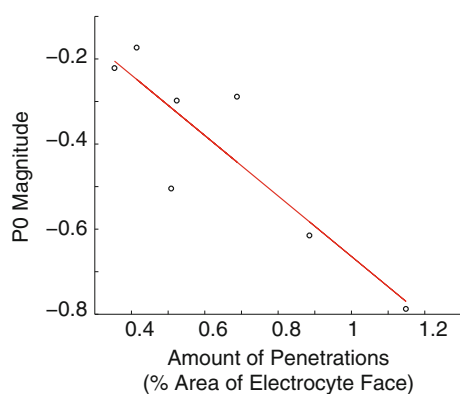


**Fig. 9** Morphological correlates of signal variation in *P. kingsleyae* electrocytes. There is a linear relationship between the percent area of electrocyte face devoted to penetrations and magnitude of P0 for seven individually dissected electrocytes ( $P = 0.008$ ;  $R^2 = 0.78$ )

appears consistent (among electrocytes with penetrations, indicated by width and color density of yellow–red bands; Fig. 7) with the individuals surveyed using serial histology (Fig. 7; Table 6).

We hypothesized that the number of penetrations is responsible for the magnitude of P0. Given that the discharge of the posterior face is responsible for P1 (Bennett 1971), we also hypothesized that delay in electrical conduction along the stalk system, after it penetrates through the electrocyte, may be responsible for the timing of P0 relative to P1. Assuming that conduction velocity along microstalklets remained constant, a source of this variation might be microstalklet territory length. We were able to determine a linear relationship between the area of electrocyte face devoted to penetrations and the magnitude of P0 (Fig. 9; slope =  $-1.10$ ;  $P = 0.008$ ;  $r^2 = 0.78$ ). Though we observed differences in the territory size, we were unable to determine any meaningful relationship between territory size and delay of P0 relative to P1.

## Discussion

*P. kingsleyae* EODs are geographically variable

Principal components analysis of EODs (Fig. 3) indicates that EOD waveforms among *P. kingsleyae* in Gabon are more similar across 21 variables (indicated by their degree of overlap) when compared to variation across these variables between other *Paramormyrops* species (Arnegard and Hopkins 2003). Despite this overall similarity, *P. kingsleyae* EOD waveforms do vary in two distinct aspects: duration and the magnitude of peak P0. Our analysis shows that this variation is clinal, and that those localities separated by the largest geographic distances are correspondingly the most divergent with respect to these

two characters; EOD duration increases from East to West, while the magnitude of P0 decreases from North to South. EOD waveforms of *P. kingsleyae* are bimodally distributed with respect to the magnitude of peak P0, corresponding to P0-absent and P0-present signal types. In the majority of the populations sampled, the P0-present signaling type was collected (Fig. 6). P0-absent individuals were collected in only two localities, at Cocobeach, and near the confluence of the Louétsi and Ngounié rivers. Both populations occur less than 10 km from P0-present populations. P0-present and P0-absent individuals rarely co-occur; only in two collection sites (Bambomo and Apassa Creeks) were P0-absent and P0-present individuals captured together.

There are several potential explanations for the observed variation in *P. kingsleyae* EOD signals. Such variation may be caused primarily by: (1) the actions of natural and/or sexual selection, (2) phenotypic plasticity coupled with variation in environmental conditions among sites, or (3) genetic drift. We consider the plausibility of each of these alternative but non-exclusive, hypotheses in light of other mormyrid studies.

**Hypothesis 1** Selection drives EOD divergence in *P. kingsleyae*

### Electroreception

EOD production serves a dual role for both communication and active electrolocation behaviors (Hopkins 1999; von der Emde 1999). The presence of an additional phase in P0-present individuals may enhance information content for electroreception because of wider frequency bandwidth per individual electric pulse, thus improving electroreceptive performance in certain conditions (Meyer 1982). We consider this an unlikely explanation since the magnitude of difference in P0 amplitude between P0-absent and P0-present waveform types is only, at maximum, 1% of the peak-to-peak amplitude of the entire EOD. In addition, our analysis of FFT curves computed for each EOD was unable to detect a systematic relationship between the presence/absence of P0 and differences in frequency content (Table 3).

### Cryptic species

Variation in EOD signals might reflect the existence of two distinct species within *P. kingsleyae*. Several lines of evidence suggest that this is unlikely: First, recent study of divergent EOD signaling in another *Paramormyrops* species has revealed, despite larger phenotypic EOD divergence in P0 magnitude, no overt evidence of reproductive isolation (Arnegard et al. 2005). Second, morphological and molecular evidence (Sullivan et al. 2002, 2004)

suggest only a single *P. kingsleyae* species rather than two distinct groups. Finally, our data suggests that the morphological differences between P0-absent and P0-present *P. kingsleyae* electric organs are not maintained in sympatry, leading to individuals of mixed morphology (Fig. 7; Table 6). This may be evidence of potential hybridization between signal types in these localities, resulting from a lack of any pre-mating reproductive isolation between the co-occurring signal types. Behavioral, neurophysiological and genetic studies are needed to completely rule out this possibility of cryptic species.

#### Character displacement

A final possibility is that of reproductive character displacement, a process of divergence which gives rise to greater courtship signal differences between co-occurring taxa than between the same taxa in geographical isolation from one another (Pfenning and Pfenning 2009). Because our collecting methods did not permit exhaustive, systematic sampling of mormyrid assemblages at multiple sites (e.g., along river channel transects), we are presently unable to rule out this possibility. We are compelled to note, however, that our collections of *P. kingsleyae* at sites in Cocobeach and creeks in the Louétsi River locality rarely included other mormyrid species. The possibility of reproductive character displacement merits future studies on the relationship between intra- and interspecific species diversity among a variety of *Paramormyrops* assemblages.

#### Hypothesis 2 Developmental Plasticity in Response to Environmental Heterogeneity Underlies EOD Variation in *P. kingsleyae*

Development of EODs and electric organs has been observed in multiple species in the laboratory (Denizot et al. 1982; Baier et al. 2006; Werneyer and Kramer 2006; Hopkins, unpublished). The P0 character emerges late in electric organ development, when larvae are approximately 2 cm in standard length, when stalk penetrations develop (Denizot et al. 1982). P0s and penetrations manifest regardless of the sex of the individual, and are retained until adulthood. Our data clearly supports that the presence or absence of P0 is not due to differences between juvenile and adult fishes, nor is it a sexually dimorphic character (Fig. 5).

Though few studies have demonstrated developmental responses of the electric organ to environmental heterogeneity (see Hopkins 1999), it is unlikely that P0 and the development of penetrations may be in response to environmental factors. Our data on *P. kingsleyae* collected from Gabon field sites 1998–2009 concerning variation in environmental variables, including water temperature, conductivity, and habitat vegetation do not predict the

variation between EOD signal types. In addition, P0s (and penetrating stalks) have widespread phylogenetic distribution (Sullivan et al. 2000; see also below), encompassing a wide variety of habitat types that have not been associated with the presence or absence of penetrating stalks. Finally, sympatric *Paramormyrops* assemblages (and other sympatric mormyrid assemblages) include P0-absent and P0-present species, presumably under the same or similar environmental influences, suggesting that the presence of P0s and penetrating stalks are more likely due to genetic differences between species.

#### Hypothesis 3 Genetic Drift within small, isolated populations Causes EOD Variation in *P. kingsleyae*

Principal components analysis revealed a strong geographic component in the described EOD variation. Because of no correlated variation in environmental conditions, and presumably few selective differences between collection localities, we consider the alternative hypothesis that distance between populations potentially explains this variation. As cartographic data were unavailable to determine river distances between many of our collection localities, we used Latitude and Longitude coordinates of our collection sites to estimate distances between populations. We found significant correlations between EOD duration and Longitude and magnitude of P0 and Latitude (Fig. 4), indicative of clinal variation in EODs across Gabon, even among temperature corrected recordings (see Online Resource 3 for more details). The clinal nature of this variation, particularly in the absence of systematic variation between populations in terms of selective or environmental factors (discussed above), leads us to favor the hypothesis that phenotypic differences may be the result of populations isolated by geographic distance. Qualitative and quantitative analysis of EODs support this (Figs. 2, 3); localities separated by the largest geographic distances (i.e. Ivindo and Upper Louétsi) are correspondingly the most divergent with respect to PC1 and PC2, whereas nearby populations are often similar (Nyanga vs. Upper Louétsi). These phenotypic differences are consistent with evidence of genetic differences between many of the same populations of *P. kingsleyae* (Sullivan et al. 2004; Arnegard et al. 2005).

We also detected spatial variation in EOD waveforms at finer geographic scales. Individuals across all populations were bimodally distributed with respect to the magnitude of peak P0, corresponding to P0-absent and P0-present signal types (Fig. 5). In the majority of the populations sampled, the P0-present signaling type was encountered (Fig. 6). P0-absent individuals were encountered in only two localities, at Cocobeach, and near the confluence of the Louétsi and Ngounié Rivers, both of which occur less than 10 km from P0-present populations. P0-present and P0-

absent individuals rarely co-occur; only in two collection sites (Bambomo and Apassa Creeks) were P0-absent and P0-present individuals captured together.

Consistent with this, both populations of P0-absent *P. kingsleyae* signal types are associated with prominent physical barriers to migration. In Cocobeach, small adjacent creeks are isolated from each other by the Atlantic Ocean, whereas along the Louétsi River, a 15 m waterfall (Bongolo Falls; Fig. 6b) isolates the Upper Louétsi from the Lower Louétsi. The distribution of signal types in the Louétsi region is consistent with Bongolo Falls acting as a barrier between populations; only P0-absent fish were collected above the Bongolo Falls ( $N = 94$ ). Bambomo Creek was one of two sites that contained both signal types. Bambomo is a tributary of a small river that drains into the Ngounié River. Its headwaters, however, are within close proximity (<150 m) of streams that ultimately drain above Bongolo Falls (Fig. 6).

Our collections have suggested that *P. kingsleyae* selectively inhabit the shallow headwaters of small creeks in many areas; as such, *P. kingsleyae* habitat preferences may reduce opportunities for migration down main river channels. Our observations of this habitat preference, taken with (1) prior evidence of genetic differences between populations over these scales (Sullivan et al. 2002, 2004; Arnegard et al. 2005) and (2) the lack of plausible selective or environmental factors that influence EOD evolution (discussed above), lead us to consider the hypothesis that divergent *P. kingsleyae* signals may have evolved as the result of reduced gene flow between populations. This may be due to large geographic distances separating some populations, across which migration is reduced, or due to more abrupt topographic changes preventing migration when prominent barriers are encountered. With such reduced gene flow, small populations of genetically isolated *P. kingsleyae*, such as those above Bongolo Falls, may have “lost” penetrating stalks and associated P0 s (see below) through the effects of genetic drift over multiple generations, during isolation from P0-present populations. While this is plausible given the lack of compelling selective pressures outlined above, we concede that more data are required concerning the population genetics of *P. kingsleyae* in this region. We are presently in the process of testing this hypothesis using microsatellite genotyping strategies among *P. kingsleyae* in the Louétsi drainage region. We note that such a mechanism has been implicated recently (via quantitative trait loci mapping) in the loss of pigmentation among the blind cave tetra *Astyanax mexicanus* (Protas et al. 2007).

#### Morphological correlates of EOD diversity

We reported two morphological features of electrocytes that are correlated with the physiological features of

waveforms: the first is the presence or absence of anteriorly innervated, penetrating stalked electrocytes (*Pa*) that are associated with P0-present or P0-absent EOD waveforms, respectively. Our analysis of 12 *P. kingsleyae* electric organs (Fig. 7; Table 6) and three-dimensional reconstruction of individual electrocytes (Fig. 8) demonstrate that these two signal types have a morphological basis. P0-present specimens have predominantly *Pa* type electrocytes whereas P0-absent specimens have electric organs with predominantly *NPP* type electrocytes. Second, we show that the presence and number of penetrating stalks (Fig. 9) is positively related to the magnitude of P0. Both findings are consistent with previous work in other mormyrid species (Bennett and Grundfest 1961; Bass 1986b).

Our analysis also detects heterogeneous electric organs, a phenomenon, to the authors’ knowledge, that has not been previously described in mormyrids. This heterogeneous morphology results from the presence of both *NPP* and *Pa* type electrocytes within the same individuals (Fig. 7). This morphological heterogeneity was only observed in specimens collected from localities where signal types occurred in close proximity (i.e. Cocobeach and Bambomo Ck.). In localities where only one signal type was found, electric organs were comparatively homogeneous. Among P0-present individuals where significant heterogeneous morphology was observed, *NPP* type electrocytes occurred only in the posterior portion of the surveyed electric organ column. Morphological heterogeneity was observed predominantly among individuals with P0-present EODs; individuals examined with P0-absent signals had comparatively homogenous *NPP* type electric organs (Fig. 7; Table 6), with occasional penetrations. *NPP* type electrocytes in heterogeneous electric organs did not occur singly, but rather occurred in discrete groups of 7–10 (Fig. 7). Denizot and Kirschbaum (1982) observed that electric organs originate in *Pollimyrus* from tail myomeres during early ontogeny, and that each myomere contributes approximately 7–10 electrocytes to the final adult organ.

Electrocyte character optimization on mormyrid phylogeny suggests that *Pa* electrocytes evolved from *NPP*-type early in the history of Mormyridae, followed by several reversals to *NPP*-type (Sullivan et al. 2000). In *Paramormyrops*, *Pa*-type were likely ancestral and there have been minimally five reversals to *NPP* in this genus alone (Sullivan et al. 2004). Stalk penetrations appear late in electrocyte ontogeny—*Pa*-type electrocytes pass through an *NPP* stage of development (Szabo 1960; Denizot et al. 1982; Hopkins unpublished). Thus, these reversals from adult *Pa*-type to *NPP*-type electrocytes have been interpreted as paedomorphic (Sullivan et al. 2004). The repeated evolutionary reversals from *Pa* to *NPP* in mormyrids and the evidence of heterogeneity in this character

**Table 6** Summary of histological analysis. Twelve electric organs were examined. Specimen numbers and localities are listed, with corresponding signal type (see “Methods”). Total numbers of electrocytes are listed, along with the number of those corresponding to *Pa* type anatomy and *NPp* type anatomy (see “Methods”)

Specimen	Locality	Signal Type	# of Electrocytes	<i>Pa</i> -type	<i>NPp</i> -type
3217	Upper Louétsi	P0-Absent	49	0	49
3170-2	Bambomo	P0-Absent	59	3	56
4025	Cocoa Beach	P0-Absent	27	2	25
N.V. “A”	Cocoa Beach	P0-Absent	58	0	58
4002	Cocoa Beach	P0-Absent	64	1	63
4020	Cocoa Beach	P0-Absent	25	0	25
2429	Libreville	P0-Present	58	58	0
2627	Mouvanga	P0-Present	60	60	0
1398	Ivindo	P0-Present	73	73	0
3170	Bambomo	P0-Present	61	39	22
4015	Cocoa Beach	P0-Present	31	21	10
3118	Bambomo	P0-Present	48	37	11

among and within populations of *P. kingsleyae* suggests that a simple genetic and developmental mechanism might underlie this character.

### Concluding remarks

Our analysis of fine-scale variation in *P. kingsleyae* EODs and electric organs provide two hypotheses concerning how EODs may evolve. First, the geographic pattern of EOD variation in *P. kingsleyae* suggest that electric signals may evolve through genetic drift, facilitated via isolation by distance, or by prominent barriers to dispersal. Second, the microevolutionary changes occurring in isolated populations of *P. kingsleyae* mirror a repeated pattern of electric organ and signal evolution in the Mormyridae as a whole. The fact that the origin of the *NPp* electrocytes and P0-absent EODs from *Pa*/P0-present ancestors is inferred to have occurred multiple times in the history of mormyrids, and again among populations of *P. kingsleyae*, suggests that the genetic mechanism controlling the development of this character may be relatively simple. In *P. kingsleyae* we may be witness to the microevolutionary, population-level processes that have contributed to the macroevolutionary patterns of signal diversity among mormyrid electric fishes.

**Acknowledgments** Permits to collect fishes in Gabon and export them for this study were granted by l’Institut de Recherche en Ecologie Tropicale, l’Institut de Recherches Agronomiques et Forestières and the Centre National de la Recherche Scientifique et Technologique. We are grateful for the valuable assistance and logistical support we received from J. D. Mbega and students working in these institutions. All techniques used are in accordance with protocols approved by Cornell University’s Center for Research Animal Resources and Education (CARE). The authors thank G. Harned for assistance with histological processing, Charles Dardia at the Cornell Museum of Vertebrates for assistance in the preparation of Online Resource 2, Cornell Microscopy and Imaging Core Facility for use of their confocal microscopy equipment. Additionally, we

thank A. McCune and K. Shaw, as well as two anonymous reviewers for comments on earlier versions of this manuscript. This work was supported by NIMH TG T32 MH015793 and NIH TG 2T32GM007469 to JRG, NIH ROI-DC6206 and NSF 0818305 to CDH, and NSF 0818390 to BAC.

### References

- Alves-Gomes J, Hopkins CD (1997) Molecular insights into the phylogeny of mormyrid fishes and the evolution of their electric organs. *Brain Behav Evol* 49:324–351
- Arnegard ME, Hopkins CD (2003) Electric signal variation among seven blunt-snouted *Brienomyrus* species (Teleostei: Mormyridae) from a riverine species flock in Gabon, Central Africa. *Environ Biol Fishes* 67:321–339
- Arnegard ME, Jackson BS, Hopkins CD (2006) Time-domain signal divergence and discrimination without receptor modification in sympatric morphs of electric fishes. *J Exp Biol* 209:2182–2198
- Arnegard ME, McIntyre PB, Harmon LJ, Zelditch ML, Crampton WGR, Davis JK, Sullivan JP, Lavoué S, Hopkins CD (2010) Sexual signal evolution outpaces ecological divergence during electric fish species radiation. *Am Nat* 176:335–356
- Arnegard ME, Bogdanowicz SM, Hopkins CD (2005) Multiple cases of striking genetic similarity between alternate electric fish signal morphs in sympatry. *Evolution* 59:324–343
- Baier B, Lamml M, Kramer B (2006) Ontogeny of the electric organ discharge in two parapatric species of the dwarf stonebasher, *Pollimyrus castelnaui* and *P. marianne* (Mormyridae, Teleostei). *Acta Zool* 87:209–214
- Bass AH (1986a) A hormone-sensitive communication-system in an electric fish. *J Neurobiol* 17:131–155
- Bass AH (1986b) Electric organs revisited: evolution of a vertebrate communication and orientation organ. In: Bullock TH, Heiligenberg W (eds) *Electroreception*. Wiley, New York, pp 13–70
- Bass AH (1986c) Species differences in electric organs of mormyrids: substrates for species-typical electric organ discharge waveforms. *J Comp Neurol* 244:313–330
- Bass AH, Denizot JP, Marchaterre MA (1986) Ultrastructural features and hormone-dependent sex-differences of mormyrid electric organs. *J Comp Neurol* 254:511–528
- Bass AH, Volman SF (1987) From behavior to membranes—testosterone-induced changes in action-potential duration in electric organs. *Proc Natl Acad Sci USA* 84:9295–9298

- Bennett MV, Grundfest H (1961) Studies on morphology and electrophysiology of electric organs III. Electrophysiology of electric organs in mormyrids. In: Chagas C, Paes de Carvalho A (eds) Bioelectrogenesis pp 113–135
- Bennett MV (1971) Electric organs. In: Hoar W, Randall D (eds) Fish physiology, vol 5. Academic Press, New York, pp 347–491
- Bradbury JW, Verencamp SL (1998) Principles of animal communication, 1st edn. Sinauer Associates, New York
- Carlson BA (2009) Temporal-pattern recognition by single neurons in a sensory pathway devoted to social communication behavior. *J Neurosci* 29:9417–9428
- Carlson BA (2002) Electric signaling behavior and the mechanisms of electric organ discharge production in mormyrid fish. *J Physiol Paris* 96:405–419
- Caputi AA, Carlson BA, Macadar O (2005) Electric organs and their control. In: Bullock TH, Hopkins C, Popper A, Fay RR (eds) Electroreception. Springer, New York, pp 410–451
- Denizot JP, Kirschbaum F, Westby GWM, Tsuji S (1982) On the development of the adult electric organ in the mormyrid fish *Pollimyrus isidori* (with special focus on the innervation). *J Neurocytol* 11:913–934
- Endler JA (1989) Conceptual and other problems in speciation. In: Otte D, Endler JA (eds) Speciation and its consequences. Sinauer Associates, Sunderland, pp 625–648
- Feulner PG, Plath M, Engelmann J, Kirschbaum F, Tiedemann R (2009) Electrifying love: electric fish use species-specific discharge for mate recognition. *Biol Lett* 23:225–228
- Foster SA, Scott RJ, Cresko WA (1998) Nested biological variation and speciation. *Philos Trans R Soc B* 353:207–218
- Xu-Friedman MA, Hopkins C (1999) Central mechanisms of temporal analysis in the knollenorgan pathway of mormyrid electric fish. *J Exp Biol* 202:1311–1318
- Günther A (1896) Report on a collection of reptiles and fishes made by Miss M.H. Kingsley during her travels on the Ogowe river and in Old Calabar. *Ann Mag Nat Hist* 100:261–285
- Hopkins CD (1980) Evolution of electric communication channels of mormyrids. *Behav Ecol Sociobiol* 7:1–13
- Hopkins CD (1986) Behavior of mormyridae. In: Bullock TH, Heiligenberg W (eds) Electroreception. Wiley, New York, pp 527–576
- Hopkins CD (1999) Signal evolution in electric communication. In: Hauser MD, Konishi M (eds) The design of animal communication. MIT Press, Cambridge, pp 461–491
- Hopkins CD, Bass AH (1981) Temporal coding of species recognition signals in an electric fish. *Science* 212(4490):85–87
- Hopkins CD, Lavoué S, Sullivan JP (2007) Mormyridae. In: Stiassny MLJ, Teugels GG, Hopkins CD (eds) Poissons D'eaux Douces Et Saumâtres De Basse Guinée: Ouest de l'Afrique Centrale vol 1. Faune Et Flore Tropicales. IRD Éditions, Paris, pp 220–334
- Iles RB (1960) External sexual differences, their significance in *Mormyrus kannume* (Forsk., 1775). *Nature* 188:516
- Kirschbaum F (1995) Reproduction and development in mormyrid and gymnotiform fishes. In: Moller P (ed) Electric fishes: history and behavior. Chapman & Hall, London, pp 267–301
- Kramer B, Westby GWM (1985) No sex difference in the waveform of the pulse type electric fish, *Gnathonemus petersii* (Mormyridae). *J Comp Physiol A* 145:399–403
- Kramer B, van der Bank H (2000) The southern churchill, *Petrocephalus wesselsi*, a new species of mormyrid from South Africa defined by electric organ discharges, genetics, and morphology. *Environ Biol Fish* 59:393–413
- Kramer B, van der Bank H, Flint N, Sauer-Gürth H, Wink M (2003) Evidence for parapatric speciation in the mormyrid fish *Pollimyrus castelnaui* (Boulenger, 1911) from the Okavango-Upper Zambezi river systems: *P. marianne* sp. nov., defined by electric organ discharges, morphology and genetics. *Environ Biol Fish* 67:47–70
- Kramer B, van der Bank H, Wink M (2004) *Hippopotamyrus ansorgii* species complex in the upper Zambezi River system with a description of a new species, *H. szaboi* (Mormyridae). *Zool Scr* 33:1–18
- Kramer B, Skelton P, van der Bank H, Wink M (2007) Allopatric differentiation in the *Marcusenius macrolepidotus* species complex in Southern and Eastern Africa: the resurrection of *M. pongolensis* and *M. angolensis*, and the description of two new Species (Mormyridae, Teleostei). *J Nat Hist* 41:647–708
- Kramer B, Swartz E (2010) *Hippopotamyrus ansorgii* complex from the Cunene river in southern Africa (Teleostei: Mormyriiformes). *J Nat Hist* 44:2213–2242
- Lamml A, Kramer B (2006) Differentiation of courtship songs in parapatric sibling species of dwarf stonebushers from southern Africa (Mormyridae, Teleostei). *Behavior* 143:783–810
- Lamml M, Kramer B (2007) Allopatric differentiation in the acoustic communication of a weakly electric fish from southern Africa, *Marcusenius macrolepidotus* (Mormyridae, Teleostei) *Behav Ecol Sociobiol* 61:385–399
- Lavoué S, Arnegard ME, Sullivan JP, Hopkins CD (2008) *Petrocephalus* of Odzala offer insights into evolutionary patterns of signal diversification in the Mormyridae, a family of weakly electrogenic fishes from Africa. *J Physiol Paris* 102:322–339
- Lévêque D, Paugy D, Teugels GG (1990) The fresh and brackish water fishes of West Africa, vol 1. Musée Royal de l'Afrique Centrale, Tervuren
- Lewontin RC (1974) The genetic basis for evolutionary change. Columbia University Press, New York
- Machnik P, Kramer B (2008) Female choice by electric pulse duration: attractiveness of the males' communication signal assessed by female bulldog fish, *Marcusenius pongolensis* (Mormyridae, Teleostei). *J Exp Biol* 211:1969–1977
- Mayr E (1963) Animal species and evolution. Belknap Press, Cambridge
- McPhail JD (1994) Speciation and the evolution of reproductive isolation in the sticklebacks (*Gasterosteus*) of southwestern British Columbia. In: Bell MA, Foster SA (eds) The evolutionary biology of the threespine stickleback. Oxford University Press, Oxford
- Meyer JH (1982) Behavioral responses of weakly electric fish to complex impedances. *J Comp Physiol A* 145:459–470
- Pezzanite B, Moller P (1998) A sexually dimorphic basal anal-fin ray expansion in the weakly discharging electric fish *Gnathonemus petersii*. *J Fish Biol* 53:638–644
- Pfenning KS, Pfenning DW (2009) Character displacement: ecological and reproductive responses to a common evolutionary problem. *Q Rev Biol* 84:253–276
- Protas M, Conrad M, Gross JB, Tabin C, Borowsky R (2007) Regressive evolution in the Mexican cave tetra, *Astyanax mexicanus*. *Curr Biol* 17:452–454
- Scheffel A, Kramer B (1997) Electrocommunication and social behavior in *Marcusenius senegalensis* (Mormyridae, Teleostei). *Ethology* 103:404–420
- Sullivan JP, Lavoué S, Arnegard ME, Hopkins CD (2004) AFLPs resolve phylogeny and reveal mitochondrial introgression within a species flock of African electric fish (Mormyroidea: Teleostei). *Evolution* 58:825–841
- Sullivan JP, Lavoué S, Hopkins CD (2000) Molecular systematics of the African electric fishes (Mormyroidea: Teleostei) and a model for the evolution of their electric organs. *J Exp Biol* 203:665–683
- Sullivan JP, Lavoué S, Hopkins CD (2002) Discovery and phylogenetic analysis of a riverine species flock of African electric fishes (Mormyridae: Teleostei). *Evolution* 56:597–616

- Szabo T (1960) Development of the electric organ of Mormyridae. *Nature* 188:760–762
- Teugels G, Hopkins CD (1998) Morphological and osteological evidence for the generic position of *Mormyrus kingsleyae* in the genus *Brienomyrus* (Teleostei: Mormyridae). *Copeia* 1998:199–204
- Verrell PA (1998) Geographic variation in sexual behavior: sex, signals and speciation. In: Foster SA, Endler JA (eds) The evolution of geographic variation in behavior. Oxford University Press, Oxford
- von der Emde G (1999) Active electrolocation of objects in weakly electric fish. *J Exp Biol* 202:1205–1215
- Werner M, Kramer B (2006) Ontogenetic development of electric-organ discharges in a mormyrid fish, the bulldog *Marcusenius macrolepidotus* (South African Form). *J Fish Biol* 69:1190–1201